Received: 10 November 2023 | Revised: 19 December 2023 | Accepted: 21 December 2023

DOI: 10.1002/jcc.27302

RESEARCH ARTICLE

Journal of COMPUTATIONAL CHEMISTRY WILEY

Application to nonlinear optical properties of the RSX-QIDH double-hybrid range-separated functional

M. Rodríguez-Mayorga[1,2] | P. Besalú-Sala[3] | Á. J. Pérez-Jiménez[1] | J. C. Sancho-García[1]

[1]Department of Physical Chemistry, University of Alicante, Alicante, Spain

[2]Université Grenoble Alpes, CNRS, Inst. NÉEL, Grenoble, France

[3]Department of Chemistry and Pharmaceutical Sciences, Amsterdam Institute for Molecular and Life Sciences (AIMMS), Vrije Universiteit Amsterdam, Amsterdam, The Netherlands

Correspondence
J. C. Sancho-García, Department of Physical Chemistry, University of Alicante, E-03080, Alicante, Spain.
Email: jc.sancho@ua.es

Funding information
Ministerio de Ciencia e Innovación, Grant/Award Number: PID2019-106114GB-I00; Vrije Universiteit Amsterdam

Abstract

The effective calculation of static nonlinear optical properties requires a considerably high accuracy at a reasonable computational cost, to tackle challenging organic and inorganic systems acting as precursors and/or active layers of materials in (nano-)devices. That trade-off implies to obtain very accurate electronic energies in the presence of externally applied electric fields to consequently obtain static polarizabilities (α_{ij}) and hyper-polarizabilities (β_{ijk} and γ_{ijkl}). Density functional theory is known to provide an excellent compromise between accuracy and computational cost, which is however largely impeded for these properties without introducing range-separation techniques. We thus explore here the ability of a modern (double-hybrid and range-separated) Range-Separated eXchange Quadratic Integrand Double-Hybrid exchange-correlation functional to compete in accuracy with more costly and/or tuned methods, thanks to its robust and parameter-free nature.

KEYWORDS
density functional theory, double-hybrid density functionals, nonlinear optical properties

1 | INTRODUCTION

The nonlinear optical response of materials strongly depends on the electronic structure of the constituent units (i.e., molecules or chromophores) and their solid-state packing or supramolecular arrangement (molecular glasses, host-guest systems, customized polymers, etc.). Therefore, the search of optimized materials by theoretical design should strongly rely on methods able to accurately calculate the electronic structure of isolated or self-organized samples. The field of nonlinear optics (NLO) have found applications in optical signal processing,[1] ultra-fast switches,[2] sensors,[3] and laser amplifiers,[4] to name just a few of them. For the deployment of new materials, gaining insights from the computational perspective can help to rationalize experimental data as well to the design of targeted candidates from scratch.[5]

However, the application of highly accurate electronic structure methods is not free from uncertainties arising from the approximations performed to alleviate the associated computational cost. The gold-standard approximation used as reference is usually a wavefunction method known as Coupled-Cluster Singles and Doubles with perturbative Triples correction, or CCSD(T), scaling as $\mathcal{O}(N^k)$, $k=7$, with respect to the system size N (the scaling is actually $\mathcal{O}(N^3M^4)$, where N is the number of electrons and M the number of basis functions). Note

P. Besalú-Sala and M. Rodríguez-Mayorga contributed equally to this work.

We would like to dedicate this work to the 60th anniversary of Carlo Adamo, whose continuous and intense work on DFT has been a longstanding example and inspiration for generations of computational chemists.

that the unfavorable $k = 7$ scaling would mean to increase the computational time by a factor 2^7 if the system size goes from N to $2N$ (e.g., from a monomer to a dimer of the same molecule) which soon becomes unaffordable for real-world systems. It has also been recently shown that application of modern numerical techniques (density fitting and/or orbital localization) can help to reduce that scaling while providing very competitive results.[6] Furthermore, the exploration of the accuracy of other low-scaling methods (e.g., $k = 3$ as the random-phase approximation) is a current line of research leading to very promising results.[7]

On the other hand, and invigorated by the excellent performance of density functional theory (DFT) for linear-response optical properties[8] or dipole moments,[9] the application of DFT to static nonlinear optical properties (SNLOPs) inherited some of the limitations (and lessons) previously found[10] to adequately select the exchange-correlation functional to be used. The most commonly applied method for those SNLOPs is probably a range-separated (semilocal or hybrid) functional, which allows to largely correct those deficiencies found before in standard calculations.[11] A further step was done by fine-tuning the range-separation value for each of the systems tackled, although at the cost of slightly increasing the associated computational time. However, despite these efforts, the accurate yet cost-effective (i.e., $k = 3-5$) calculation of hyper-polarizabilities is still a matter of ongoing work.

Therefore, we will here assess the application of one of the most sophisticated range-separated functionals currently existing in DFT, after merging exchange and correlation effects from wavefunction-based methods with parameter-free exchange and correlation density functional, a.k.a. double-hybrid density functionals.[12,13] Some previous (yet limited) investigations have shown the ability of these double-hybrid functionals to accurately predict dipole moments[14] or polarizabilities.[15] Similarly to range-separated hybrid models, the question of how to fix the range-separation value is also solved for the assessed model by imposing an exact (universal) constraint, leading thus to a completely non-empirical model (Range-Separated eXchange Quadratic Integrand Double-Hybrid [RSX-QIDH], *vide infra*) deserving to be still assessed for this kind of challenging systems, which is thus the main purpose of this work. We would also like to remark that the thorough assessment of double-hybrid density functionals done along the last years, including their benchmarking across the whole GMTKN55 dataset,[16] is mostly done for thermochemical and/or kinetics properties, and thus not for the properties here targeted.

2 | THEORETICAL FRAMEWORK

2.1 | Computation of SNLOPs

Provided an externally applied electric field $\mathbf{F}$ is small in magnitude, the molecular response (i.e., its dipole moment μ) will be linearly proportional to its strength, or simply $\mu_i = \alpha_{ij}F_j$, with α_{ij} being the linear polarizability of the molecule. If the electromagnetic interactions becomes more intense, the induced polarization obeys a nonlinear dependence with respect to the electric field strength. In such a case, the Taylor-like series expansion of the field-dependent dipole moment[17] $\boldsymbol{\mu}(\mathbf{F})$ or energy[18] $E(\mathbf{F})$ gives rise to:

$$E(\mathbf{F}) = E(\mathbf{0}) - \sum_i \mu_i F_i - \frac{1}{2!}\sum_{ij}\alpha_{ij}F_iF_j - \frac{1}{3!}\sum_{ijk}\beta_{ijk}F_iF_jF_k - \frac{1}{4!}\sum_{ijkl}\gamma_{ijkl}F_iF_jF_kF_l + \cdots \tag{1}$$

with i,j,k,l being any Cartesian component (i.e., x,y, or z) and the expansion coefficients,

$$\mu_i = -\frac{\partial E}{\partial F_i}\Big|_{\mathbf{F}=\mathbf{0}}, \tag{2}$$

$$\alpha_{ij} = -\frac{\partial^2 E}{\partial F_i \partial F_j}\Big|_{\mathbf{F}=\mathbf{0}}, \tag{3}$$

$$\beta_{ijk} = -\frac{\partial^3 E}{\partial F_i \partial F_j \partial F_k}\Big|_{\mathbf{F}=\mathbf{0}}, \tag{4}$$

$$\gamma_{ijkl} = -\frac{\partial^4 E}{\partial F_i \partial F_j \partial F_k \partial F_l}\Big|_{\mathbf{F}=\mathbf{0}}, \tag{5}$$

identified respectively as the dipole moment, the static polarizability, the first hyper-polarizability, and the second hyper-polarizability.

2.2 | The RSX-QIDH model

The Range-Separated eXchange (RSX-) Quadratic Integrand Double-Hybrid (QIDH) functional[19] combines an EXact-eXchange term E_x^{EXX} and a Perturbative-like second order correlation correction E_c^{PT2} to the exchange-correlation functional components $E_x[\rho]$ and $E_c[\rho]$, taking the form:

$$\begin{aligned} E_{xc}^{\mathrm{RSX-QIDH}}[\rho] &= a_x E_x^{\mathrm{EXX}} + (1-a_x)E_x^{\mathrm{EXX}}(\omega) + (1-a_x)E_x[\rho] \\ &\quad -(1-a_x)E_x[\rho](\omega) + a_c E_c^{\mathrm{PT2}} + (1-a_c)E_c[\rho], \end{aligned} \tag{6}$$

as a function of the range-separation ω value.[20] The coefficients a_x and a_c are non-empirically determined and borrowed from the original (non-range-separated) QIDH model,[21] being thus $a_x = 3^{-1/3}$ and $a_c = 1/3$. The source of the RSX-QIDH expression comes from splitting the two-electron operator into short- and long-range terms,

$$\frac{1}{r_{ij}} = \frac{1-\left[\alpha+\beta f(\omega r_{ij})\right]}{r_{ij}} + \frac{\alpha+\beta f(\omega r_{ij})}{r_{ij}}, \tag{7}$$

with f being the error function allowing to analytically solve all the Gaussian-based integrals needed for the calculation.[22,23] The preservation of the non-empirical nature of the RSX-QIDH model needs also to identify $\alpha = a_x$ and $\beta = 1-\alpha$, together with an additional condition to fix the ω value: $\omega = 0.27$ bohr^{-1} for RSX-QIDH after imposing the recovery of the total energy of the H atom.[24,25] When the PBE

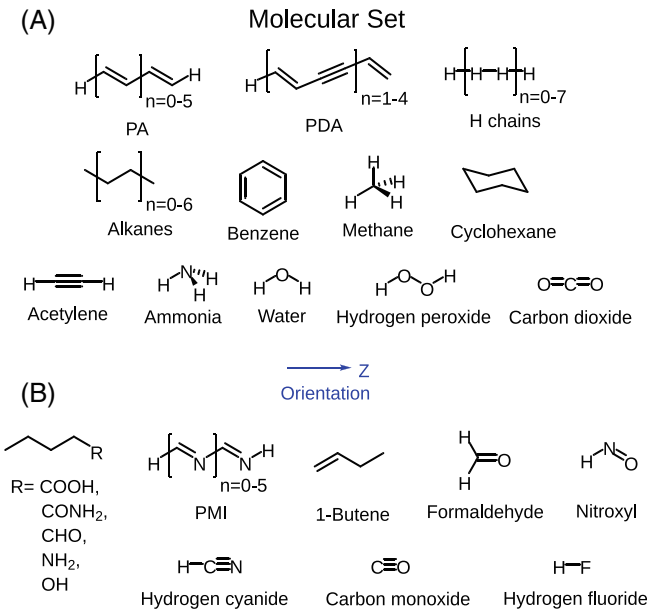

FIGURE 1 Chemical structures of the molecular subsets employed in this study, including the orientation of the applied electric field.

exchange and correlation functionals[26] are also used, the RSX-(PBE-)QIDH (a.k.a. RSX-QIDH) functional is completely defined.

2.3 | Computational details

The set of molecules tackled are presented in Figure 1, which includes 50 medium-sized (organic and inorganic) representative systems whose selection is based on: (i) the availability of reference results obtained previously at the CCSD(T) level, and (ii) the possible comparison with other previously assessed methods[7] to adequately bracket their accuracy with respect to RSX-QIDH. The whole set is divided into subset A, for those systems presenting vanishing odd derivatives (i.e., $\mu_z = \beta_{zzz} = 0$) due to their inversion symmetry with respect to the electric field, and subset B, composed by molecules with all (even and odd) non-vanishing energy derivatives. The geometries of the compounds are taken from Reference 27 as they were optimized at the MP2/aug-cc-pVDZ (subset A) and CCSD/aug-cc-pVDZ (subset B) level. Note that the set of systems selected also comprises representative π-conjugated oligomers, such as all-*trans* polyacetylene (PA), all-*trans* poly-methyneimine (PMI), and polydiacetylene (PDA) of varying size, which allows us to compare the results as a function of the oligomer size, as well as challenging hydrogen chains[28] for which the monomer bond length and the distance between adjacent monomers were set so that the oligomers do not present strong non-dynamic correlation. All the calculations are done with the aug-cc-pVDZ basis set[29] and the corresponding aug-cc-pVDZ-RI auxiliary basis set, using the latest release of the `MOLGW`code,[30,31] implementing double-hybrid density functionals belonging to the QIDH family, for which the RSX-QIDH functional has been specifically added for this work using the `libxc`library.[32,33]

The electronic dipole moments and (hyper)polarizabilities were calculated numerically as consecutive derivatives of the electronic energy with respect to the external electric field, thus using the finite field approach. Specifically, the range of electric fields used was $F = \pm 2^i \times 10^{-4}$ a.u. where the index i ranges from 0 to 8. The truncation error affecting the numerical estimation of the derivatives originated by the higher-order terms is neglected in the standard central-differentiation formulation. To minimize it, we made use of the standard Rutishauser–Romberg scheme.[34,35] The associated Rutishauser–Romberg errors are also reported in the Supporting Information.

3 | RESULTS AND DISCUSSION

Seen in the past the good performance of range-separated hybrid functionals, we will here compare the results of our RSX-QIDH calculations with the following best-performer methods:

1. The LC-BLYP[22] functional with its default $\omega = 0.47$ bohr^{-1} value, which showed before[11] a reasonable quality for (hyper-)polarizabilities than other range-separated functionals commonly employed such as ωB97XD[36] or CAM-B3LYP.[23] Other studies[37,38] showed how this functional performs well for γ_{zzzz} but generally poorly for β_{zzz} compared to other range-separated and hybrid density functional approximations such as CAM-B3LYP, ω B97XD, or M06-2X.
2. The Tα-LC-BLYP[11] functional, but with a fine-tuned ω value (and thus system-dependent) adapted to the closest as possible reproduction of the CCSD(T) values for γ_{zzzz}.

Additionally, we will also consider the following alternatives to cover the range of high-quality available methods:

1. The RPA@PBEh(0.85) method, which employs the random-phase approximation[39–41] for the correlation energy, together with the orbitals arisen from a DFT calculations employing a hybrid functional (PBEh) with an EXX proportion of $a_x = 0.85$ (see Reference 7 for further details about the construction of this method).
2. The pristine PBE-QIDH functional, without the corresponding range-separation scheme but preserving the same $a_x = 3^{-1/3}$ and $a_c = 1/3$ coefficients of RSX-QIDH, to assess the influence of the latter technique on the performance of double-hybrid functionals.

In other words, we plan to benchmark the latest RSX-QIDH with respect to CCSD(T), concomitantly comparing its performance with respect to that of the best candidates arising from previous studies, thus discarding other range-separated functionals, wavefunction methods, or RPA-based variants. Note also that the cost and formal scaling $\mathcal{O}(N^k)$ of the set of methods compared here ranges from $k = 3$ of RPA@PBEh(0.85) to $k = 5$ of PBE-QIDH and RSX-QIDH, with LC-BLYP and Tα-LC-BLYP lying at the intermediate ($k = 4$) point. For the comparison of the values between the methods tested, we will use

TABLE 1 Error metrics for the predicted (hyper)-polarizabilities compared to CCSD(T) values[a].

Property		LC-BLYP	Tα-LC-BLYP	RPA@PBEh(0.85)	PBE-QIDH	RSX-QIDH
μ_z	MAE	1.57E−01	1.19E−01	1.11E−01	1.16E−01	1.46E−01
	RMSE	2.48E−01	1.96E−01	1.91E−01	1.98E−01	2.41E−01
	MAX	6.75E−01	5.31E−01	4.95E−01	5.22E−01	6.60E−01
	MEAN%	21.15	18.47	13.59	13.88	20.18
	MAX%	48.75	67.11	52.45	46.36	85.93
α_{zz}	MAE	7.16E+00	9.61E+00	5.34E+00	1.23E+01	7.88E+00
	RMSE	1.35E+01	1.75E+01	1.09E+01	2.76E+01	1.63E+01
	MAX	4.81E+01	6.30E+01	4.29E+01	1.26E+02	6.17E+01
	MEAN%	4.56	5.66	3.07	5.45	4.25
	MAX%	16.19	13.15	9.73	20.38	13.98
β_{zzz}	MAE	1.34E+02	1.01E+02	1.42E+02	5.23E+01	1.35E+02
	RMSE	3.82E+02	2.77E+02	3.48E+02	1.40E+02	3.83E+02
	MAX	1.50E+03	1.11E+03	1.24E+03	5.56E+02	1.49E+03
	MEAN%	61.14	73.59	49.35	39.20	49.42
	MAX%	413.13	433.48	121.21	258.14	265.56
γ_{zzzz}	MAE	4.06E+04	1.88E+04	6.58E+04	1.51E+05	3.48E+04
	RMSE	9.22E+04	5.85E+04	2.60E+05	6.31E+05	1.15E+05
	MAX	3.43E+05	3.22E+05	1.64E+06	4.16E+06	7.32E+05
	MEAN%	19.44	5.92	13.90	19.13	14.43
	MAX%	50.73	29.32	49.50	78.46	27.59

[a]CCSD(T) and (Tα-)LC-BLYP values taken from Reference 11 and RPA@PBEh(0.85) and PBE-QIDH values taken from Reference 7.

the mean absolute error (MAE), the root-mean-squared error (RMSE), the MAXimum Error (MAX) (all in a.u.) and the MEAN relative errors (MEAN%) and MAXimum relative errors (MAX%) with respect to the CCSD(T) calculated values.

Table 1 gathers the error metrics for all the methods here considered and for the μ_z, α_{zz}, β_{zzz}, and γ_{zzzz} properties, with the individual values for each molecule and method given as part of the Supplementary Material. Looking first at μ_z, RSX-QIDH does not fully meet the quality of PBE-QIDH, the latter actually competes in accuracy with RPA@PBEh(0.85), but it becomes competitive with respect to range-separated hybrid functionals such as LC-BLYP, Tα-LC-BLYP, or ωB97XD (see the Supplementary Material for results with the latter method). Note that: (i) the good performance of double-hybrid functionals was also part of the conclusions of the study conducted[9] by Head-Gordon et al. over a database comprising dipole moments for 150 molecules; (ii) parameter-free double-hybrid methods are also known to perform better for electric-induced properties than parameterized ones[42,43]; and (iii) PBE-QIDH is known to outperform[7] other double-hybrid functionals such as (parameterized) B2PLYP[44] and (parameter-free) PBE0-DH[45] for all polarizabilities and hyperpolarizabilities. Overall, for this property, methods that present different theoretical backgrounds display qualitatively similar results, therefore cheaper methods would be recommended over expensive ones in this situation. It is important to remark here that some molecules in the studied set present very small dipole moments and therefore tiny changes in their predicted value might induce large changes in relative errors. Therefore, it is maybe more interesting, for this property, to focus on the absolute error indicators. In this regard, PMI6 is the oligomer causing the MAX error for all methods, illustrating the size-dependency of the properties which will also be later analyzed in more detail.

Considering now α_{zz} values, the RPA@PBEh(0.85) method is the best performer followed closely by RSX-QIDH and the rest of the methods for both relative and absolute error indicators. It is therefore the recommended method closely followed by LC-BLYP and RSX-QIDH. However, there is no method rendering qualitatively incorrect results. Nevertheless, for α_{zz}, the larger errors come from the PDA oligomers, and the ability to reduce these has a large impact on the MEAN% and the MAE and RSME. The β_{zzz} (γ_{zzzz}) errors are increased in all cases with respect to μ_z (α_{zz}), as it usually happens with numerical derivatives, with RSX-QIDH matching or improving the errors provided by PBE-QIDH, and slightly outperforming other range-separated hybrid functionals for β_{zzz}. While μ_z and α_{zz} are linear properties which are, in general, predicted properly by most methods, the non-linear β_{zzz} and γ_{zzzz} are usually trickier to predict. In this regard, for β_{zzz}, the newer alternatives, namely RPA@PBEh(0.85), RSX-QIDH, and specially PBE-QIDH, improve over the Tα-LC-BLYP range-separated hybrid functional, which we remind here that was fined-tuned for γ_{zzzz}, at the cost of increasing the computational time. Moving to γ_{zzzz} the fine-tuned Tα-LC-BLYP is still the best among all the tested

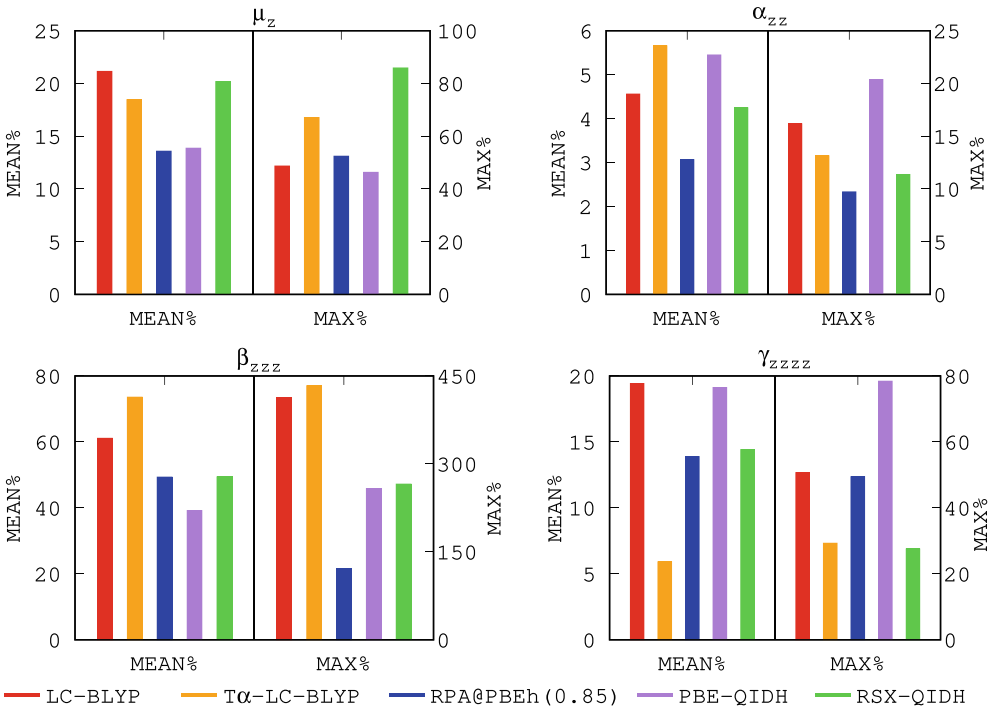

FIGURE 2 Mean relative errors (MEAN%) and maximum relative errors (MAX%) for (hyper)-polarizabilities, as obtained by several methods compared with CCSD(T) reference values.

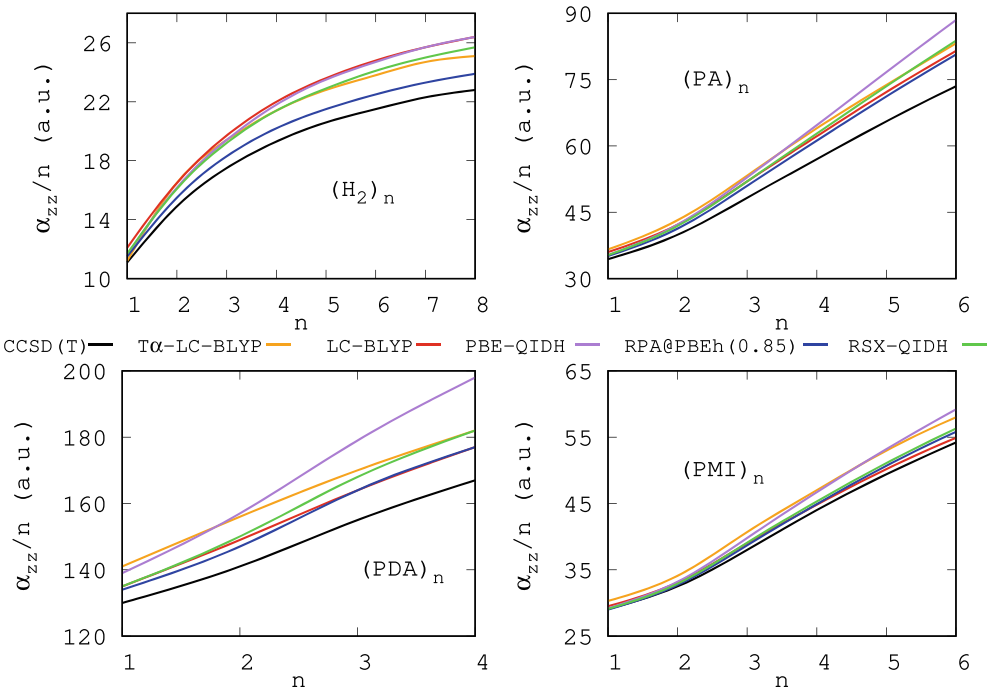

FIGURE 3 α_{zz} values (normalized per number of monomers) versus the number of monomers (n) for hydrogen chains, PA, PDA, and PMI.

methods (not surprisingly, as it has been designed to tackle this property specifically). Among the non-tuned methods, RSX-QIDH and LC-BLYP perform with quite good results, with the latter being less computationally demanding. On the other hand, RPA@PBEh(0.85) still emerges as a robust and accurate alternative. Not surprisingly, in all the cases the systems with higher errors are also those bearing larger properties, that is, the longer oligomers of PDA and PMI. Thus, a note regarding the design of new methods: it seems thus crucial to be able to describe properly the larger oligomers for a method to become robust towards NLOP predictions.

Figure 2 shows the evolution of the MEAN% and MAX% values among the methods considered, basically ranking their quality as a function of the property targeted. Overall, RSX-QIDH can be seen as behaving slightly better than PBE-QIDH for α_{zz} and γ_{zzzz} and being of similar accuracy for β_{zzz}, taken also into account that PBE-QIDH was already more accurate than other double-hybrid density

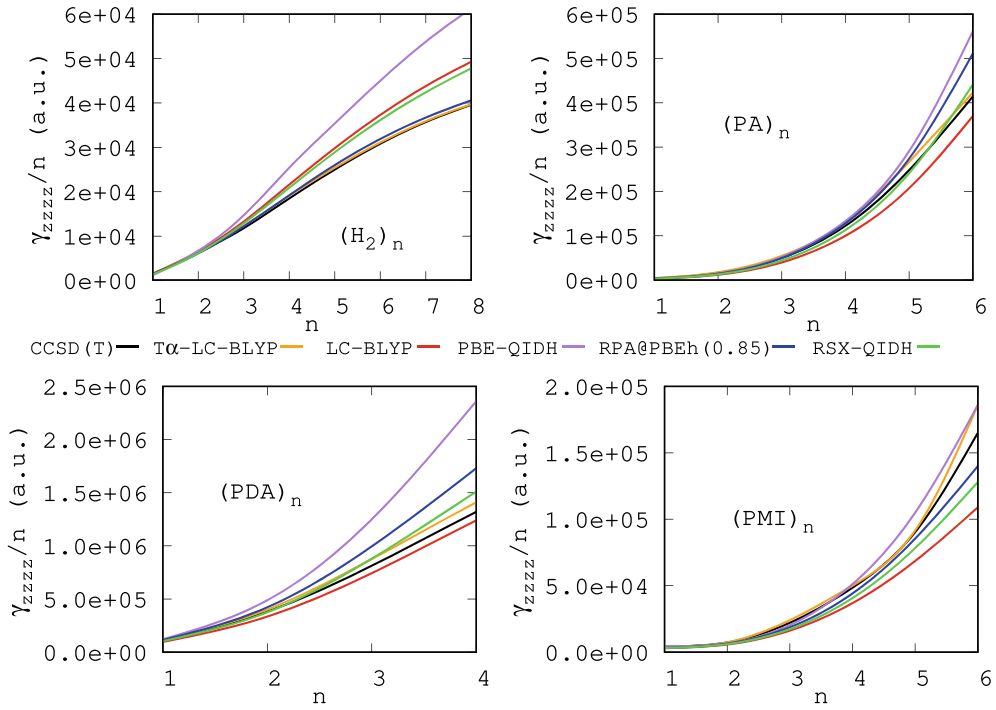

FIGURE 4 γ_{zzzz} values (normalized per number of monomers) versus the number of monomers (n) for hydrogen chains, PA, PDA, and PMI.

functionals previously assessed.[7] However, this was not the case for μ_z for which the error by RSX-QIDH is non-negligible. Additionally, the performance of the RPA@PBEh(0.85) method is also encouraging, depending on the availability of its due implementations in the existing codes, since it provides a very competitive accuracy with respect to any other method but at a reduced computational cost (once the work of setting the details of the method was previously afforded by the authors[7]).

The evolution of the results with the system size can be inferred for the error metrics calculated for hydrogen chains, as well as the PA, PDA, and PMI oligomers, since those chemical components of the dataset formed adding sequential units as $(H_2)_n$, $(PA)_n$, $(PDA)_n$, and $(PMI)_n$ would thus allow to estimate the quality of the results with respect to the system size n. Figure 3 displays the evolution of α_{zz} values versus n, indicating not only if the property is expected to saturate with the system size but also how the different methods can reproduce the shape and slope of the curve given at the CCSD(T) level. In all cases, the comparison of RSX-QIDH with PBE-QIDH favors the former, likely due to the reduced self-interaction error of RSX-QIDH compared to other methods. Note that RSX-QIDH has provided very accurate values for energy-based properties of other size-dependent systems assessed before, such as increasingly longer $(He)_n^+$ clusters[19] or C_n nanorings,[46] with the performance here remarking its quality. Similarly to α_{zz}, Figure 4 shows the evolution of γ_{zzzz} values versus n for the same $(H_2)_n$, $(PA)_n$, $(PDA)_n$, and $(PMI)_n$ systems. Once again, RSX-QIDH leads to curves closer to CCSD(T) than PBE-QIDH, generally speaking. Interestingly, the performance of the RPA@PBEh(0.85) method is remarkably accurate too, thus situating this methods as one of the most robust so far tested after its comparison with best-performers range-separated hybrid and double-hybrid methods.

4 | CONCLUSIONS

We have assessed in this work the performance of the range-separated double-hybrid functional RSX-QIDH for μ_z, α_{zz}, β_{zzz}, and γ_{zzzz} magnitudes, compared with that of highly accurate methods belonging to various and diverse families such as LC-BLYP, Tα-LC-BLYP, RPA@PBEh(0.85), and PBE-QIDH. To this end, we have relied on CCSD(T) benchmark results, allowing thus to estimate the performance of all the methods based on metrics such as the MAE, the RMSE, the MAX and the MEAN relative errors (MEAN%) and MAXimum relative errors (MAX%) with respect to those CCSD(T) reference values. The quality of the results obtained by RSX-QIDH seems very promising, as well as those of the pristine PBE-QIDH models on which is it based, taken into account their fully non-empirical nature due to the absence of any implicit or explicit parameterization, contrarily to other range-separated density functionals. However, their computational scaling needs to also be considered for tackling larger systems, which could also be alleviated by introducing localization techniques for their perturbative component (e.g., DLPNO-MP2[47]). The previously developed RPA@PBEh (0.85) model[7] still keeps a very accurate performance compared with RSX-QIDH, at a lower computational cost. Therefore, this study allows any user to rationally choose an accurate method depending mostly on: (i) their availability in computational codes; and (ii) the size of the system to be studied.

ACKNOWLEDGMENTS

The work in Alicante is supported by the "Ministerio de Ciencia e Innovación" of Spain (Grant No. PID2019-106114GB-I00). P. B.-S. acknowledges the financial support received from the Vrije Universiteit Amsterdam. The authors thank Éric Brémond (U. Paris Cité) for

discussions regarding the implementation of the RSX-QIDH model in the code used.

DATA AVAILABILITY STATEMENT

The data that supports the findings of this study are available within the article (and its Supporting Information) or are available from the corresponding authors upon reasonable request.

ORCID

M. Rodríguez-Mayorga https://orcid.org/0000-0003-0869-9787
P. Besalú-Sala https://orcid.org/0000-0002-0955-9762
Á. J. Pérez-Jiménez https://orcid.org/0000-0002-1276-7255
J. C. Sancho-García https://orcid.org/0000-0003-3867-1697

REFERENCES

[1] A. Astill, *Thin Solid Films* **1991**, *204*, 1.
[2] C. Quémard, F. Smektala, V. Couderc, A. Barthelemy, J. Lucas, *J. Phys. Chem. Solids* **2001**, *62*, 1435.
[3] D. Gounden, N. Nombona, W. E. Van Zyl, *Coord. Chem. Rev.* **2020**, *420*, 213359.
[4] D. Mace, M. Adams, *Europhys. News* **1987**, *18*, 48.
[5] F. Castet, C. Tonnelé, L. Muccioli, B. Champagne, *Acc. Chem. Res.* **2022**, *55*, 3716.
[6] C. Naim, P. Besalú-Sala, R. Zaleśny, J. M. Luis, F. Castet, E. Matito, *J. Chem. Theory Comput.* **2023**, *19*, 1753.
[7] P. Besalú-Sala, F. Bruneval, Á. J. Pérez-Jiménez, J. C. Sancho-García, M. Rodríguez-Mayorga, *J. Chem. Theory Comput.* **2023**, *19*, 6062.
[8] C. Adamo, D. Jacquemin, *Chem. Soc. Rev.* **2013**, *42*, 845.
[9] D. Hait, M. Head-Gordon, *J. Chem. Theory Comput.* **2018**, *14*, 1969.
[10] A. J. Cohen, P. Mori-Sánchez, W. Yang, *Chem. Rev.* **2012**, *112*, 289.
[11] P. Besalú-Sala, S. P. Sitkiewicz, P. Salvador, E. Matito, J. M. Luis, *Phys. Chem. Chem. Phys.* **2020**, *22*, 11871.
[12] L. Goerigk, S. Grimme, *Wiley Interdiscip. Rev.: Comput. Mol. Sci.* **2014**, *4*, 576.
[13] E. Brémond, I. Ciofini, J. C. Sancho-García, C. Adamo, *Acc. Chem. Res.* **2016**, *49*, 1503.
[14] A. Mohajeri, M. Alipour, *J. Chem. Phys.* **2012**, *136*, 124111.
[15] M. Alipour, *J. Phys. Chem. A* **2014**, *118*, 5333.
[16] L. Goerigk, A. Hansen, C. Bauer, S. Ehrlich, A. Najibi, S. Grimme, *Phys. Chem. Chem. Phys.* **2017**, *19*, 32184.
[17] P. Pulay, *Wiley Interdiscip. Rev.: Comput. Mol. Sci.* **2014**, *4*, 169.
[18] M. Nakano, I. Shigemoto, S. Yamada, K. Yamaguchi, *J. Chem. Phys.* **1995**, *103*, 4175.
[19] E. Brémond, M. Savarese, Á. J. Pérez-Jiménez, J. C. Sancho-García, C. Adamo, *J. Chem. Theory Comput.* **2018**, *14*, 4052.
[20] D. Tozer, *J. Chem. Phys.* **2003**, *119*, 12697.
[21] É. Brémond, J. C. Sancho-García, Á. J. Pérez-Jiménez, C. Adamo, *J. Chem. Phys.* **2014**, *141*, 031101.
[22] H. Iikura, T. Tsuneda, T. Yanai, K. Hirao, *J. Chem. Phys.* **2001**, *115*, 3540.
[23] T. Yanai, D. P. Tew, N. C. Handy, *Chem. Phys. Lett.* **2004**, *393*, 51.
[24] É. Brémond, Á. J. Pérez-Jiménez, J. C. Sancho-García, C. Adamo, *J. Chem. Phys.* **2019**, *150*, 201102.
[25] É. Brémond, Á. J. Pérez-Jiménez, J. C. Sancho-García, C. Adamo, *J. Chem. Phys.* **2020**, *152*, 244124.
[26] J. P. Perdew, K. Burke, M. Ernzerhof, *Phys. Rev. Lett.* **1996**, *77*, 3865.
[27] Molecular Properties Virtual lab, https://molprolab.com/data/ (accessed: June 5, 2023).
[28] A. Ruzsinszky, J. P. Perdew, G. I. Csonka, G. E. Scuseria, O. A. Vydrov, *Phys. Rev. A* **2008**, *77*, 060502.
[29] T. H. Dunning Jr., *J. Chem. Phys.* **1989**, *90*, 1007.
[30] F. Bruneval, T. Rangel, S. M. Hamed, M. Shao, C. Yang, J. B. Neaton, *Comput. Phys. Commun.* **2016**, *208*, 149.
[31] MOLGW code, http://www.molgw.org (accessed: April 10, 2023).
[32] M. A. Marques, M. J. Oliveira, T. Burnus, *Comput. Phys. Commun.* **2012**, *183*, 2272.
[33] S. Lehtola, C. Steigemann, M. J. Oliveira, M. A. Marques, *SoftwareX* **2018**, *7*, 1.
[34] H. Rutishauser, *Numer. Math.* **1963**, *5*, 48.
[35] M. Medveď, M. Stachová, D. Jacquemin, J.-M. André, E. A. Perpete, *J. Mol. Struct.: THEOCHEM* **2007**, *847*, 39.
[36] J.-D. Chai, M. Head-Gordon, *J. Chem. Phys.* **2008**, *128*, 084106.
[37] L. Lescos, S. P. Sitkiewicz, P. Beaujean, M. Blanchard-Desce, B. Champagne, E. Matito, F. Castet, *Phys. Chem. Chem. Phys.* **2020**, *22*, 16579.
[38] C. Naim, F. Castet, E. Matito, *Phys. Chem. Chem. Phys.* **2021**, *23*, 21227.
[39] D. C. Langreth, J. P. Perdew, *Phys. Rev. B* **1977**, *15*, 2884.
[40] M. Fuchs, X. Gonze, *Phys. Rev. B* **2002**, *65*, 235109.
[41] F. Furche, T. Van Voorhis, *J. Chem. Phys.* **2005**, *122*, 164106.
[42] M. Alipour, *J. Phys. Chem. A* **2013**, *117*, 4506.
[43] M. Alipour, *Chem. Phys. Lett.* **2016**, *644*, 163.
[44] S. Grimme, *J. Chem. Phys.* **2006**, *124*, 034108.
[45] E. Brémond, C. Adamo, *J. Chem. Phys.* **2011**, *135*, 024106.
[46] E. Brémond, A. Pérez-Jiménez, C. Adamo, J.-C. Sancho-Garcia, *Phys. Chem. Chem. Phys.* **2022**, *24*, 4515.
[47] E. Brémond, H. Li, J. C. Sancho-García, C. Adamo, *J. Phys. Chem. A* **2022**, *126*, 2590.

SUPPORTING INFORMATION

Additional supporting information can be found online in the Supporting Information section at the end of this article.

How to cite this article: M. Rodríguez-Mayorga, P. Besalú-Sala, Á. J. Pérez-Jiménez, J. C. Sancho-García, *J. Comput. Chem.* **2024**, *45*(13), 995. https://doi.org/10.1002/jcc.27302